ELSEVIER

Catalysis Today 42 (1998) 101–116

CATALYSIS TODAY

Chemical, structural and mechanistic aspects on NO_x SCR over commercial and model oxide catalysts

Luca Lietti[a,*], Gianguido Ramis[b], Francesco Berti[c], Giampietro Toledo[c], Davide Robba[c], Guido Busca[b], Pio Forzatti[a]

[a]*Dipartimento di Chimica Industriale ed Ingegneria Chimica "G. Natta", Politecnico di Milano, Piazza L. da Vinci 32, 20133 Milano, Italy*
[b]*Istituto di Chimica, Facoltà di Ingegneria, Università, P.le Kennedy, I-16129 Genova, Italy*
[c]*ENEL s.p.a., DSR/CRAM, Via Rubattino 54, I-20134 Milano, Italy*

Abstract

The chemico-physical characteristics and the catalytic activity of commercial and home-made V_2O_5–WO_3/TiO_2 catalysts has been investigated in this work. The samples are constituted by TiO_2 anatase that supports the V and W components (and S in the case of commercial catalysts). The V+W estimated surface coverage is below that corresponding to the theoretical monolayer, but when surface sulfates are also taken into account the monolayer capacity of the samples is exceeded. V, W and sulfates are present on the dry catalyst surface in the form of isolated vanadyl, wolframyl and sulfate species, all in a mono-oxo-type form.

The adsorption–desorption study showed that NO does not adsorb on the catalyst surface, whereas NH_3 adsorbs on both Lewis and Brønsted acid sites. Lewis-bonded NH_3 species are thermally more stable than ammonium ions, and upon heating, a weak band is observed at 1540 cm^{-1}, that has been assigned to an amide species NH_2. When a NH_3-covered surface is heated in the presence of NO, ammonia is activated on Lewis acid sites and then reacts with gas-phase NO to give N_2.

Mechanistic features of the selective catalytic reduction (SCR) reaction have also been collected by means of transient methods, including the temperature programmed desorption/reaction techniques and the transient response analysis (TRA). These experiments proved that: (i) the reaction occurs between adsorbed ammonia and gas-phase or weakly adsorbed NO; (ii) NH_3 can not only adsorb over the active V-sites but also on the surface W- and Ti-sites and on surface sulfates as well, hence acting as an ammonia ''reservoir''; (iii) the mechanism is of the redox type, i.e. oxygen oxidizes the surface sites reduced by the other reactants. A mechanistic model for the SCR reaction has thus been derived that is consistent with our data and with literature indication as well.

Keywords: Selective catalytic reduction; V_2O_5–WO_3/TiO_2 catalysts; NO+NH_3 reaction; SCR mechanism

1. Introduction

DeNO$_x$ing of flue gases from stationary sources is efficiently achieved by using the so-called SCR (selective catalytic reduction) process. Ammonia injected in the flue gases is used as the reducing agent for NO following the reaction:

$$4NH_3 + 4NO + O_2 \Rightarrow 4N_2 + 6H_2O \quad (1)$$

This technology first developed in Japan in 1970s is widely applied worldwide. The industrial catalysts for

*Corresponding author. Tel.: 2-23993272; fax: 2-70638173; e-mail: lietti@axp7000.cdc.polimi.it

0920-5861/98/$32.00
PII S0920-5861(98)00081-9

the SCR process are based on V_2O_5–WO_3/TiO_2 or V_2O_5–MoO_3/TiO_2 oxides [1,2]. Several studies have been published concerning the characterization of V_2O_5–WO_3/TiO_2 model and the commercial SCR catalysts [3–9]. Also, the mechanism of this reaction and the role of the catalysts components have been addressed by different research groups (e.g. [10–15]). In particular, there is now a general agreement on the fact that the active sites for the SCR are associated to V centers, although V_2O_5 is usually present in small amounts in the typical catalyst formulation, and that NO reacts from the gas-phase or a weakly adsorbed state with a strongly adsorbed and activated ammonia molecule. However, several aspects concerning the chemical and mechanistic features of the SCR reaction are still under debate.

The present paper provides a critical survey of the most recent and relevant data obtained in our laboratories on the characterization of the catalyst bulk and surface structures and on the identification of the mechanistic features of the reaction mechanism over commercial and model V_2O_5–WO_3/TiO_2 catalysts. In particular, the following aspects have been addressed: (i) the chemico-physical characteristics of the commercial catalysts in comparison with those of model samples; (ii) the nature of the adsorbed ammonia species present on the catalyst surface; (iii) their role and reactivity in the SCR reaction; (iv) the role of the V, W and Ti components in the reaction mechanism and on the catalyst reactivity.

2. Experimental

2.1. Materials

Commercial and home-made catalysts have been used in the present study. Commercial catalysts were obtained as powder by crushing commercial honeycomb samples. Reference model catalysts have been prepared either by impregnating home-made TiO_2 anatase with ammonium paratungstate and/or ammonium metavanadate solutions [3,16] or by using commercial pure or sulfated ($\approx$1% w/w sulfates) TiO_2 and WO_3/TiO_2 powder (Bayer) impregnated with a solution of NH_4VO_3. The WO_3 loading was nearly 10% (w/w) whereas the V_2O_5 content was varied in the range 0–2% (w/w).

2.2. Characterization techniques

Surface area and pore size distribution measurements, XRD analysis and FT-IR spectra were obtained as described elsewhere [3,4]. Surface analysis of the commercial catalysts by XPS was performed by using a Leybold-Haereus EA11 electron energy analyzer and Al K_α X-ray radiation. Elemental analysis of the same catalysts was performed by X-ray fluorescence (with a Philips PW 1400 instrument) for Ti, W, Si, Al, Ca, and K and by atomic absorption spectroscopy (ICP) for Mo, V, Na, Mg, Al, Fe, Ba, Pb, Cr, Cu, Mn, Sr, Ni, Zn and K with a Spectraflame spectrometer. SEM–EDS analyses were performed with a Jeol JSM-840 A instrument.

2.3. Reactivity measurements

Steady-state catalytic activity runs as well as transient reactivity experiments (temperature programmed desorption–reaction studies and step changes in the SCR reactants) have been performed in a quartz tubular fixed bed microreactor (i.d. 6 mm) containing 160 mg of the catalyst (60–100 mesh). The outlet of the reactor is connected to both a quadrupole mass detector (UTI model 100 C) and a gas chromatograph for analysis of the gases exiting the reactor. Steady-state catalytic activity runs have been performed by using a stream containing 800 ppm NH_3+800 ppm NO+O_2 (1% v/v) in He (total flow rate=60 N cm^3/min). The following mass to charge (*m*/*e*) ratios were used to monitor the concentration of products and reactants: 17 (NH_3), 18 (H_2O), 28 (N_2), 30 (NO), 32 (O_2), 44 (N_2O) and 46 (NO_2). The mass spectrometer data were quantitatively analyzed by using the fragmentation patterns and the response factors were determined experimentally from calibration gases. The interference of H_2O on *m*/*e* 17 and of N_2O on *m*/*e* 28 and 30 was taken into account in determining the products composition.

Nitrogen balances, performed on the gases exiting from the reactor under steady-state conditions, were always close within $\pm$5%.

Transient reactivity experiments have been performed by imposing stepwise perturbations (0$\rightarrow$700 ppm and 700$\rightarrow$0 ppm) in the NH_3 (or NO) reactor inlet concentration while keeping constant the concentrations of the other reactants and the overall

flow rate, which was maintained at 120 N cm^3/min. A four-port valve was used to perform the abrupt switches and care was taken in minimizing all possible dead volumes in the lines before and after the reactor and in eliminating pressure and flow changes upon switching of the reactants. The dead time measured for an inert tracer (Ar) was in the order of 2 s, and was found negligible with respect to the characteristic times of the measured responses. The concentration of products and reactants was monitored as described in the case of steady-state experiments. Further details on the experimental equipment and procedure can be found elsewhere [16–18].

3. Results and discussion

3.1. Bulk chemical analyses and surface XPS analysis of commercial catalysts

In Table 1 the bulk (measured by chemical analyses) and the surface (performed by XPS) molar compositions of a V_2O_5–WO_3/TiO_2 commercial catalyst are reported and compared. XPS analysis gives V, W and S amounts higher than chemical analysis, confirming their preferential location at the surface. In contrast, the Ti surface amount is lower than the bulk composition as expected. It is also worth noticing that both analyses show the presence of components like Si, Al, Fe, alkali and alkaline earth cations, that are not expected on/in catalyst particles. Actually, the presence of siliceous materials is also very evident in the IR skeletal analysis through the detection of a quite strong band in the range 1300–1000 cm^{-1}, attributed to the Si–O–Si asymmetric stretching. SEM and TEM analyses clearly show that the catalyst particles are mixed with morphologically very different glass-like particles.

Table 1
Elemental and surface analyses of a commercial V_2O_5–WO_3/TiO_2 catalyst

Element	Bulk analysis		XPS surface analysis (% mol/mol)
	% (w/w)	% (mol/mol)	
O	Balance	64.4	66.2
Ti	48.9	28.1	25.5
V	0.26	0.1	0.2
W	7.17	1.1	3.6
Mo	—	—	—
S	∼1[a]	0.8	1.0
Si	3.36	3.2	3.4
Mg	0.11	0.1	0.7
Al	0.84	0.9	Traces
Ca	0.96	0.7	—
Fe	0.1	0.05	—
Na	0.01	0.02	—
K	0.03	0.02	—

[a]Evaluated from TG analysis.

By assuming that the catalyst particles only contain O–T–W–V–S, the bulk composition of a catalyst particle is 0.5% V_2O_5, 3.2% SO_4^{2-}, 9.6% WO_3, and 86.7% TiO_2. If one considers that vanadium and tungsten oxides and sulfate ions are exclusively located at the catalyst surface, and taking into account the measured surface area of the commercial catalyst (70 m^2/g), the coverage of the titania support particles can be estimated. According to literature data, one WO_3 formal molecule occupies 24×10^{-2} nm^2 [19], while one V_2O_5 formal molecule covers 20.83×10^{-2} nm^2 [20]: the estimated TiO_2 surface coverage is thus 93%. On the other hand, by assuming that all the sulfates are present on the catalyst surface, the sulfate surface coverage correspond to ∼30% of the theoretical monolayer. Hence the W+V+sulfates coverage exceeds the monolayer capacity of the catalyst particle.

3.2. Surface structures of model and commercial catalysts

The nature of the surface species of both homemade and commercial V_2O_5–WO_3/TiO_2 catalyst samples has been, in all cases, investigated by FT-IR and Raman spectroscopy.

In Fig. 1 the spectrum of a pressed disk of the commercial catalyst (spectrum a) is compared with that of a model V_2O_5–WO_3–TiO_2 catalyst prepared using sulfated titania as the support (spectrum b) in the region 2200–1000 cm^{-1}. The spectra have been recorded after outgassing at 623 K. The spectrum of the commercial sample shows clear bands at 2045, 2015 and 1375 cm^{-1}, that are also present in the spectrum of the model catalyst. These bands are always present in the spectra of TiO_2-based catalysts containing V_2O_5, WO_3 and sulfates, respectively. The first two bands have been demonstrated to be due to the first overtones of the V=O and W=O stretching

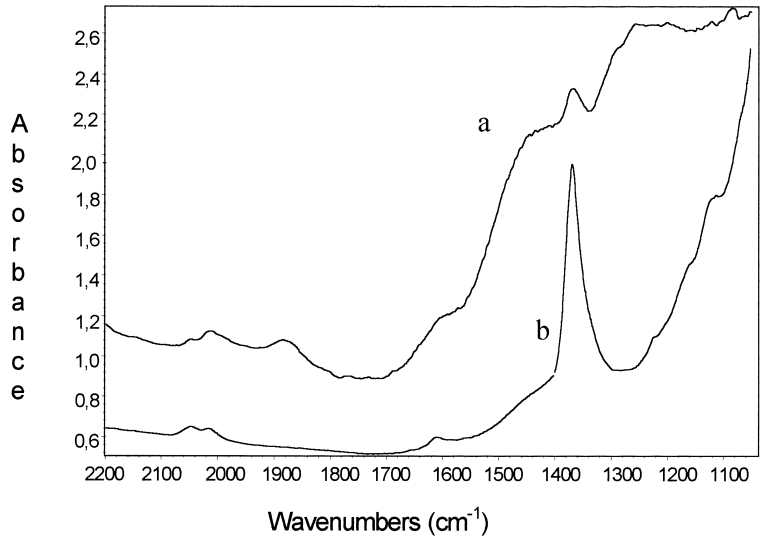

Fig. 1. FT-IR spectra of pressed disks of a commercial catalyst (a) and of a model V_2O_5–WO_3/TiO_2 catalyst (b) prepared with sulfated titania, both outgassed at 673 K.

modes of surface vanadyl and wolframyl centers, respectively. On the other hand, the band at 1375 cm^{-1} is due to the S=O stretching of surface sulfate species. These characteristic features in the spectra confirm the presence of isolated vanadyl species, isolated wolframyl species and sulfate species, all in a mono-oxo-type form on dry surfaces like those shown in the Scheme 1.

Besides the spectrum of the commercial catalyst shows a weak band at 1890 cm^{-1}, and a cut-off limit near 1300 cm^{-1}. The model catalysts do not present such features, and the cut-off limit is near 980 cm^{-1}. These additional features are associated to the siliceous particles cited above, that are also associated to a sharp band at 3745 cm^{-1} (not shown in the spectra) due to the Si–OH silanol groups (ν_{OH}).

The spectrum of the commercial catalyst is also compared in Fig. 2 with those of a model V_2O_5–TiO_2 catalyst, a model WO_3–TiO_2 catalyst and a model V_2O_5–WO_3–TiO_2 catalyst with 1:1 V:W atomic ratio. It is interesting to note that the bands of the first overtones of the V=O and W=O surface bonds have approximately the same intensity. On the contrary, the commercial catalyst shows an integrated intensity of

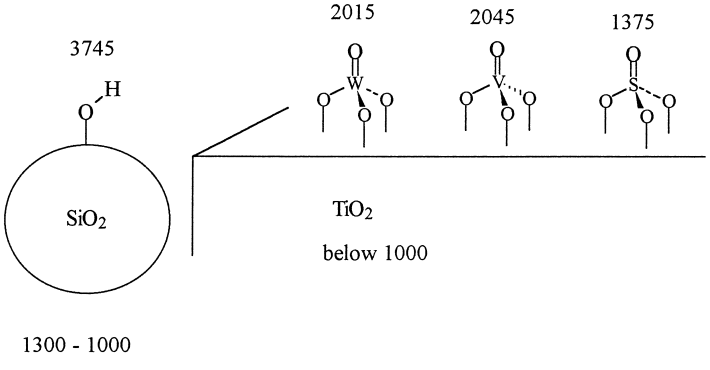

Scheme 1. Structure of the surface species present in the case of the commercial V_2O_5–WO_3–TiO_2 catalyst. The numbers in the scheme represent the correspondent IR absorption frequencies (cm^{-1}).

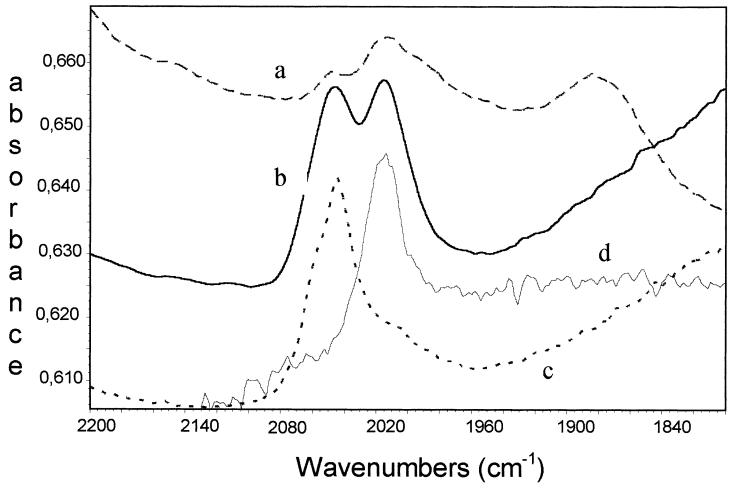

Fig. 2. FT-IR spectra of pressed disks of (a) commercial SCR catalyst; (b) a model V_2O_5–WO_3–TiO_2 catalyst (V:W atomic ratio 1:1); (c) a model V_2O_5–TiO_2 catalyst; (d) a model WO_3–TiO_2 catalyst, all after outgassing at 673 K.

the W=O stretching mode that is much higher than that of the V=O stretching mode. The ratio between the integrated areas of the two peaks is nearly 10, that compares well with the W/V molar ratio measured by chemical analysis.

The IR spectra recorded after adsorbing water and basic probe molecules (ammonia and pyridine) show that vanadyl and wolframyl species are strongly perturbed upon adsorption as demonstrated by the shift of the bands at 2045 and 2015 cm^{-1}, respectively. This shows that the above vanadyl and wolframyl sites can act as Lewis acid sites being formally coordinatively unsaturated. In wet atmospheres part of vanadyl and wolframyl species are hydrated, giving rise to structures like those shown in Scheme 2, where M=V or W. These hydrated species are characterized by bands in the region 980–950 cm^{-1} ($\nu_{V=O}$ and/or $\nu_{W=O}$).

The IR spectra of adsorbed CO_2 shows that the impregnation of TiO_2 with increasing amount of vanadia, tungsta and/or sulfates causes the disappearance of the nucleophilic sites that are able to adsorb CO_2 in the form of carbonates and bicarbonates. On the industrial catalyst such species are not formed at all, showing that these sites are completely neutralized by the surface species. This confirms that the titania surface is covered by a complete ''monolayer'' of surface complexes that involve the reaction of the surface oxide ions of titania with V-, W- and S-oxide species. This does not exclude that coordinatively unsaturated Ti cations can still remain exposed in part at the surface.

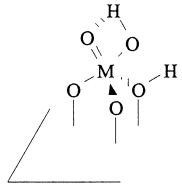

Scheme 2. Structures of the hydrated surface species present in the case of model and commercial V_2O_5–WO_3/TiO_2 samples.

3.3. Adsorption–desorption of the SCR reactants

The interaction of the reactants of the SCR reaction, i.e. NH_3 and NO, has been also investigated in our labs.

In the case of NO adsorption, the IR spectra does not allow to detect any adsorbed species from NO on the activated commercial and model V_2O_5–WO_3–TiO_2 catalysts, if very pure NO gas is used, contact is relatively slow (30 min) and the catalyst contains sufficient V, W and S to approach the monolayer coverage.

A completely different situation is apparent in the case of NH_3 adsorption. In this case, the FT-IR spectra relative to the adsorption of ammonia on the commercial catalysts are shown in Fig. 3. The presence of

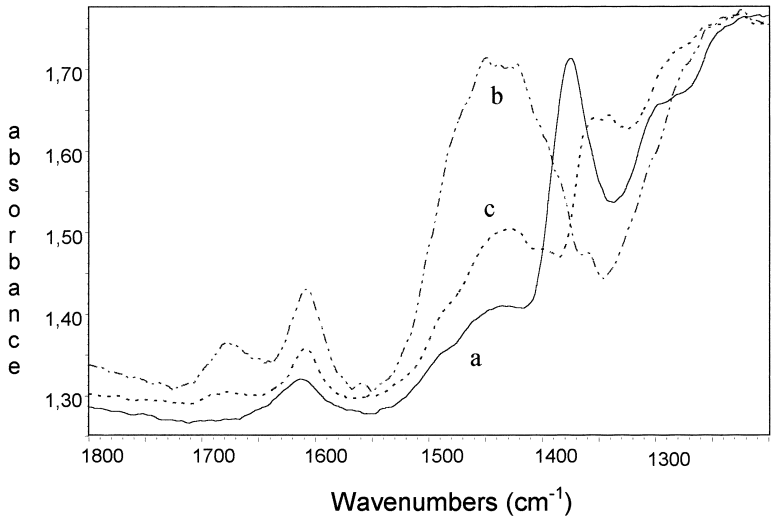

Fig. 3. FT-IR spectra of a pressed disk of a commercial catalyst after outgassing at 673 K (a), after contact with ammonia 5 Torr and a brief outgassing at r.t. (b) and after further outgassing at 423 K (c). The band at 1375 cm^{-1} (sulfate species) is perturbed upon NH_3 adsorption.

sulfates and silica does not allow the inspection of the region below 1400 cm^{-1} that is perturbed or obscured. However, the spectra of the adsorbed species are virtually identical to those observed on silica-free and sulfate-free V_2O_5–WO_3–TiO_2 model catalysts (like that shown in Fig. 4, spectrum a). The spectra shown in Figs. 3 and 4(d) indicate that both Lewis and Brønsted sites are located at the catalysts surfaces, giving rise to two strongly adsorbed species which can have the structures shown in Scheme 3.

The species coordinated on Lewis sites (species a), associated with Ti-, V- and W-oxide surface species, are characterized by bands in the region 3500–3100 (ν_{NH}), 1600 (δ_{as,NH_3}) and 1300–1150 cm^{-1} (δ_{sym,NH_3}), while the protonated species formed on Brønsted W–OH and/or V–OH sites are characterized by bands in the regions 3000–2600 (ν_{NH}), 1680 (δ_{sym,NH_4}) and 1445 cm^{-1} (δ_{as,NH_4}). Sulfate species not only provide strong Brønsted acidity but also increase the strength of the Lewis sites for inductive effects.

Outgassing at progressively higher temperatures causes the progressive faster disappearance of the bands of protonated ammonia (ammonium ions) and the slower disappearance of the bands of coordinated ammonia, which are still detectable at above 673 K. These data show that ammonia is more strongly bonded on Lewis than on Brønsted sites.

It is also worth noting that a component could be observed at 1540 cm^{-1} upon heating. A possible assignment for this very weak band is the NH_2 scissoring mode of an amide species, which is similar but not identical to that already observed at 1485 cm^{-1} in the case of WO_3/TiO_2 samples and at 1550 cm^{-1} for V_2O_5/TiO_2 catalysts [21,22]. It is concluded that also on the ternary catalysts the activation of ammonia possibly occurs through the amide species.

Temperature programmed desorption (TPD) experiments performed over the model V_2O_5–WO_3/TiO_2 samples [14] confirm that NO does not adsorb to a significant extent whereas NH_3 is strongly adsorbed over the catalyst surface. The NH_3-TPD spectra appear very broad, thus indicating the presence of several ammonia adsorbed species. The NH_3 desorption is completed only above 773 K and a small fraction of adsorbed ammonia is oxidized to N_2 and NO, possibly via the amide species detected by FT-IR spectroscopy.

3.4. *Reactivity studies and mechanistic aspects of the SCR reaction*

3.4.1. *FT-IR analysis*

The reaction of adsorbed ammonia with NO has been investigated by FT-IR, and the spectra recorded

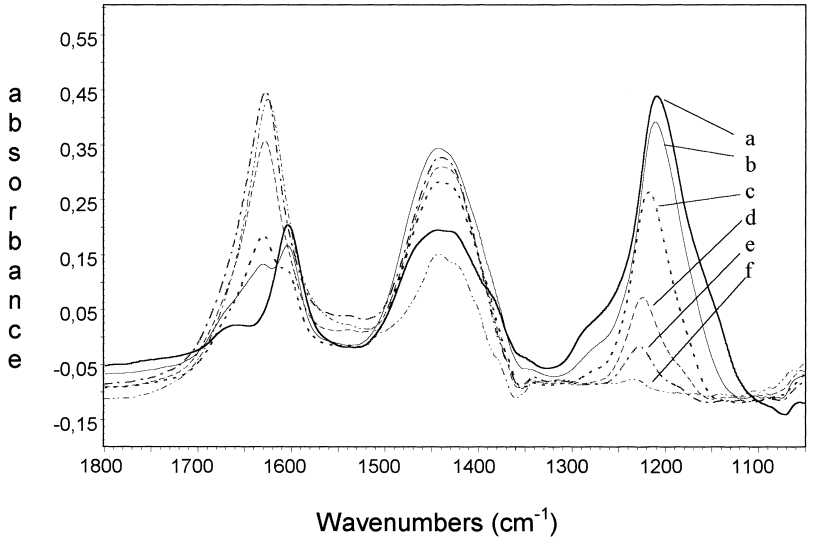

Fig. 4. FT-IR spectra of the adsorbed species arising from the interaction of NO (10 Torr) with adsorbed ammonia on a model V_2O_5–WO_3–TiO_2 catalyst, at different temperatures: (a) 300 K; (b) 373 K; (c) 403 K; (d) 423 K; (e) 453 K; (f) 523 K.

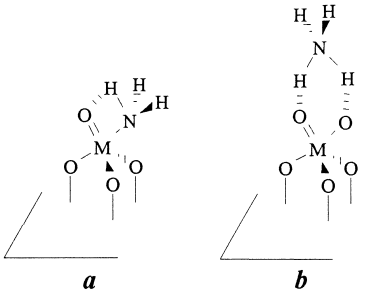

Scheme 3. Structures of ammonia bonded to Lewis (a) and Brønsted (b) acid sites.

during the reaction of NO with NH_3 on a model V_2O_5–WO_3–TiO_2 catalyst are shown in Fig. 4. It is evident that contact of the ammonia-covered surface with NO gas at temperatures above 373 K causes the progressive decrease of the asymmetric and symmetric deformation modes of coordinated ammonia (1600 and 1300–1100 cm^{-1}, respectively). Concomitantly, the scissoring mode of water (1630 cm^{-1}) appears and grows progressively. The main band of ammonium ion (1450 cm^{-1}) instead, first apparently grows, but later begins to decrease too, although slowly. When coordinated ammonia is almost gone, bands of ammonium ions also tend to disappear progressively.

The behavior with temperature of adsorbed ammonia in the presence of NO thus contrasts with that observed in the absence of NO (Fig. 3), where the bands corresponding to the ammonium ion species disappeared first. Accordingly these data suggest that ammonia is activated on Lewis acid sites and then reacts with gas-phase NO to give N_2. The involvement of Lewis-bonded coordinated ammonia in the SCR reaction has also recently been proved by performing the NH_3+NO reaction over other samples (e.g. Cu-, Fe- and Mn-based catalysts) that are also active in SCR but with lower selectivity to N_2 with respect to V_2O_5-based catalysts [23,24]. Indeed these catalysts do not present Brønsted acidity, and accordingly this observation supports the involvement of Lewis acid sites in the SCR reaction. The results obtained upon adsorption of other N-containing molecules (e.g. hydrazine, hydroxylamine) are consistent with the hypothesis that ammonia is activated on these SCR-active catalysts in the form of amide species, which can later either react with NO to give N_2 via the SCR reaction or dimerize to hydrazine finally giving N_2 by selective oxidation of ammonia [23].

3.4.2. TPSR and TPR

Mechanistic aspects of the SCR reaction between adsorbed ammonia and gas-phase NO have also been investigated by means of the temperature programmed desorption/reaction methods, e.g. temperature programmed surface reaction (TPSR) of pre-adsorbed ammonia with gaseous NO and temperature programmed reaction (TPR) of NH_3+NO. The advantage of such techniques is that by operating under transient conditions, the sequence of steps involved in the reaction could be analyzed.

The reactivity of pre-adsorbed ammonia with gas-phase NO has been investigated at first. Upon heating under a flow of He+800 ppm NO (containing also trace amounts of oxygen) a model V_2O_5–WO_3/TiO_2 catalyst sample (V_2O_5 and WO_3=1.47 and 9% (w/w), respectively; S_a=80 m^2/g, estimated V, W and Ti coverage=0.12, 0.67 and 0.21, respectively), that has been previously saturated with NH_3 (TPSR experiment), the occurrence of the SCR reaction could be monitored through the consumption of NO (trace *a* of Fig. 5(A)) and the simultaneous formation of nitrogen and water (not reported in the figure). The onset of the SCR reaction is already evident at low temperatures, below 100°C, and is indicated in Fig. 5(A) as T_{SCR}. The NO conversion increases with temperature, shows a maximum near 350°C and then decreases due to the depletion of adsorbed ammonia surface species. As shown in Fig. 5(B), the consumption of impure oxygen contained in the feed stream is also evident, starting from 200°C (T_{OX}). A comparison of T_{SCR} (∼100°C) with T_{OX} (∼200°C) clearly shows that gas-phase oxygen is involved in the SCR reaction only at temperatures well above those corresponding to the onset of the SCR reaction. This observation indicates that at low temperatures below T_{OX}, the SCR reaction involves the participation of the catalyst lattice oxygen, thus leading to catalyst reduction. Indeed it is unlikely that the catalyst is reoxidized by NO at such low temperatures. At high temperatures, above T_{OX}, gaseous oxygen is involved in the catalyst reoxidation process. These data confirm that the SCR reaction occurs via a redox mechanism that involves at first the participation of the catalyst lattice oxygen leading to catalyst reduction, followed by catalyst reoxidation by gas-phase oxygen.

These experiments have also been performed in the presence of high oxygen concentrations, namely 1% (v/v). The NO conversion obtained in this case is reported as trace *b* in Fig. 5(A). The oxygen concentration trace has not been reported due to the high O_2 content. A comparison of trace *b* with trace *a* shows that the onset of the SCR reaction (i.e. T_{SCR}) is rather unaffected by the presence of oxygen; higher NO conversion are measured only at higher temperatures, above 150–200°C. As in the case of the experiments performed in the presence of trace amounts of oxygen (trace *a*), the NO conversion shows a maximum (near 250°C) due to the depletion of adsorbed ammonia species.

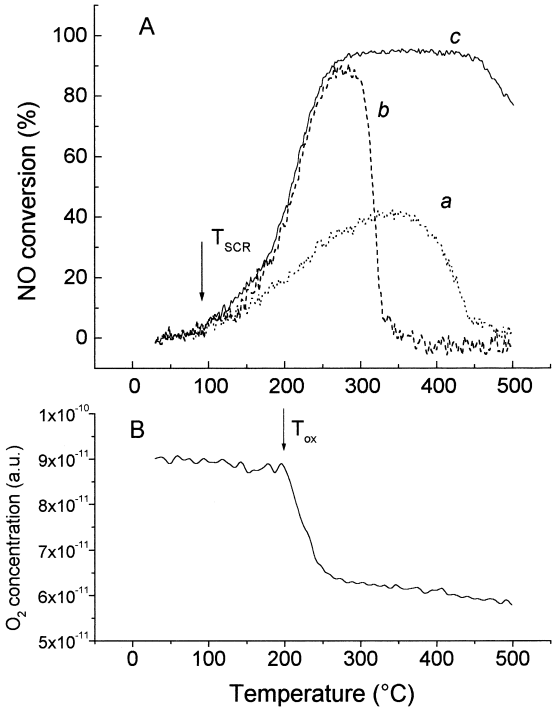

Fig. 5. (A) Results of NO-TPSR experiments in He+NO (800 ppm)+O_2 (oxygen in trace amount: trace *a*; oxygen 1% v/v: trace *b*) and of NO-TPR experiments in He+NO (800 ppm)+NH_3+O_2 1% v/v (trace *c*) performed over a model V_2O_5–WO_3/TiO_2 catalyst sample (V_2O_5 and WO_3=1.47 and 9% w/w, respectively). (B) Oxygen consumption in the case of the NO-TPSR experiment performed in the presence of trace amounts of oxygen.

The results obtained in the presence of 1% (v/v) oxygen confirm the redox mechanism of the SCR reaction previously suggested. Indeed, in line with the role of oxygen in a redox mechanism, the tem-

perature threshold of the SCR reaction (T_{SCR}) is not significantly affected by the oxygen concentration in the gas-phase, being related to the catalyst reducibility. On the other hand, oxygen does accelerate the rate of reaction at higher temperatures (near T_{OX}), by increasing the rate of the catalyst reoxidation.

The role of gas-phase ammonia in the catalyst reactivity has also been investigated. For this purpose, an experiment has been performed by heating the same catalyst sample under a flow of He+NO (800 ppm)+NH_3 (800 ppm) in the presence of 1% (v/v) oxygen (TPR experiment). The NO conversion measured in this case is reported as trace *c* in Fig. 5(A), where it is compared with the results of TPSR experiments reported above (trace *b*). It appears that the NO conversion is unaffected by the presence of NH_3 in the gas-phase up to 300°C. At higher temperatures, the NO conversion measured in the case of the TPR experiment is higher than that measured during the corresponding TPSR experiments as expected. Indeed during the TPR experiment ammonia is continuously fed to the catalyst as opposed to TPSR experiments where NH_3 is pre-adsorbed on the catalyst surface at the beginning of the run. Accordingly, these results clearly indicate that (i) due to the high acidity of the catalyst sample, high ammonia surface coverage are guaranteed in the low temperature region even in the absence of gas-phase ammonia, and (ii) the rate of the SCR reaction is not affected by the ammonia surface coverage (θ_{NH3}) for θ_{NH3} values above a characteristic critical value. These points will be further addressed in the following section.

TPSR and TPR experiments have also been performed with catalyst samples having different V_2O_5 and WO_3 loading [25]. It has been observed that the reactivity of the catalysts in the SCR reaction is increased by either increasing the vanadia or the tungsta loading, since higher NO conversions are achieved at lower temperatures. As a matter of fact, both the temperature of the onset of the SCR reaction (T_{SCR}) and the catalyst reoxidation temperature (T_{OX}) decreases either by increasing the V and/or the W loading [26]. This might be interpreted as an increase of the redox properties of the catalyst samples, being T_{SCR} and T_{OX} indicative of the catalyst reduction and reoxidation processes, respectively. This explanation is also in line with a previous characterization study showing that WO_3 addition increases the redox properties of V_2O_5/TiO_2 catalysts [3,27].

3.4.3. Steady-state catalytic activity runs

The reactivity of various V_2O_5–WO_3/TiO_2 submonolayer catalyst samples having different V and/or W loading has also been investigated by steady-state activity runs. In line with the results of the transient reactivity study, the reactivity in the SCR reaction significantly increases on increasing either the V and/or the W loading. Fig. 6 shows the vanadium TOFs (V-TOFs) for the SCR of NO with NH_3 estimated at 227°C over two series of catalyst samples

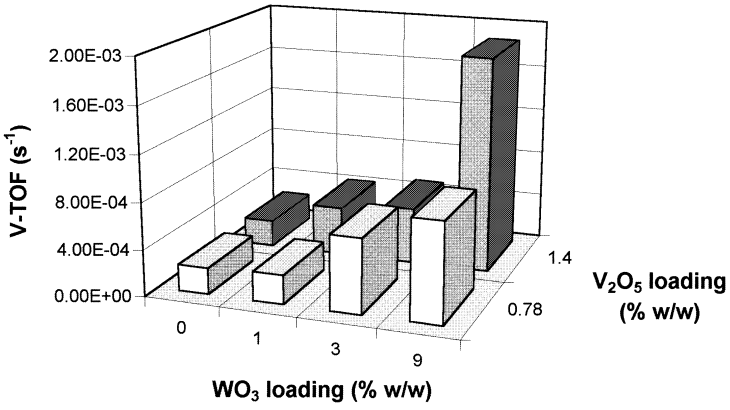

Fig. 6. Vanadium TOFs (V-TOFs) for the SCR of NO with NH_3 estimated at 227°C over two series of catalyst samples having V_2O_5 loading of 0.78% (w/w) and 1.47% (w/w), respectively, and different WO_3 amounts (in the range 0–9% w/w). Experimental conditions: see Section 2.

having V_2O_5 loading of 0.78 and 1.47% (w/w), respectively, and different WO_3 amounts (in the range 0–9% w/w). At this temperature, the N_2 selectivity is 100% over all catalyst samples. Fig. 6 clearly shows that the SCR TOFs increase with increasing vanadia loading or upon addition of tungsta. The TOF values reported in Fig. 6 are very similar to those reported by Wachs et al. [10] over TiO_2-supported V_2O_5 and V_2O_5–WO_3 catalysts. Similar results have also been reported by other authors, and the observed increases in the V-TOFs have been explained by invoking different factors. These include the increase of the catalyst redox properties [7,13], the formation of new Brønsted acid sites [5], the requirement of a dual-site mechanism for the SCR reaction [10] or of an acid and a redox catalyst function [15]. Our characterization data [3,27] along with the results of the transient reactivity experiments, showing a decrease of T_{SCR} and T_{OX} upon increasing the V_2O_5 and/or the WO_3 loading, apparently point out an increase of the redox characteristics of the samples. However, a dual-site mechanism and/or the involvement of both acid and redox functions cannot be ruled out.

3.4.4. Transient response analysis (TRA)

To gain additional information concerning the mechanistic features of the $DeNO_x$ reaction, the TRA method has been applied to both the study of the adsorption–desorption of the SCR reactants (NH_3 and NO) and of the dynamics of the SCR reaction over both a binary V_2O_5/TiO_2 and a ternary V_2O_5–WO_3/TiO_2 catalyst. This has been performed by imposing stepwise perturbations in the reactant inlet concentrations over different catalysts and at different temperatures. When the NH_3 (or NO) inlet concentration is changed stepwise in $He+O_2$, the adsorption/desorption characteristics of the single reactants can be secured; on the other hand, when the NH_3 (or NO) inlet concentration is varied in $He+NO$ (or NH_3)$+O_2$ the dynamics of the SCR reaction can be analyzed. Detailed mechanistic information could be obtained by the analysis of the reactor outlet concentration profiles of the SCR reactants and products following the stepwise changes of the inlet reactant concentration.

The adsorption–desorption characteristics of the reactants have been addressed at first, over the same catalyst sample used for TPSR/TPR measurements (i.e. a V_2O_5–WO_3/TiO_2 model catalyst with V_2O_5=1.47% w/w and WO_3=9% w/w). Typical results obtained in the case of NH_3 and NO adsorption and desorption following step changes in the NH_3 or NO reactor inlet concentration in $He+O_2$ are shown in Fig. 7(A) (adsorption) and Fig. 8(A) (desorption). The reactant ideal inlet step is also reported as a dashed line. In the case of NO adsorption–desorption (squares), Fig. 7(A) and Fig. 8(A) show that the outlet NO reactor concentration closely resembles the ideal inlet concentration (dotted line). Furthermore, the NO response is practically superimposed to that of an inert

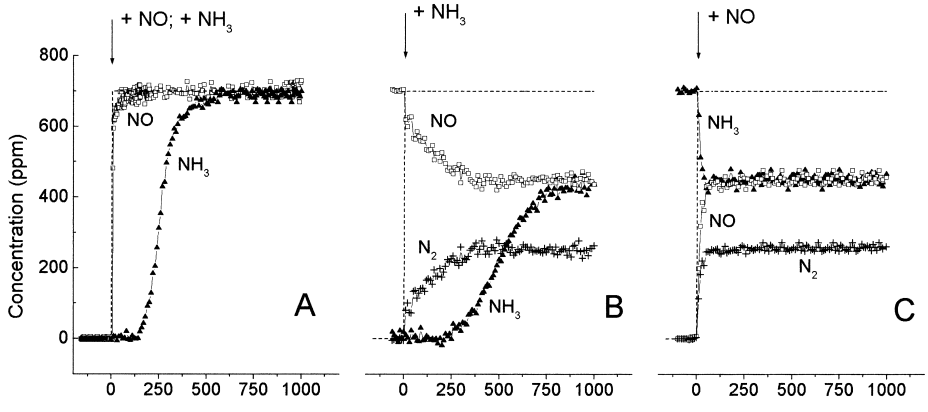

Fig. 7. Results of TRA performed over a V_2O_5–WO_3/TiO_2 model catalyst with V_2O_5=1.47% (w/w) and WO_3=9% (w/w). (A) Positive step addition of NO in $He+O_2$ and of NH_3 in $He+O_2$. (B) Positive step addition of NH_3 in $He+NO+O_2$. (C) Positive step addition of NO in $He+NH_3+O_2$. Experimental conditions: see Section 2. Dotted lines: ideal step; squares: NO; triangles: NH_3; crosses: N_2.

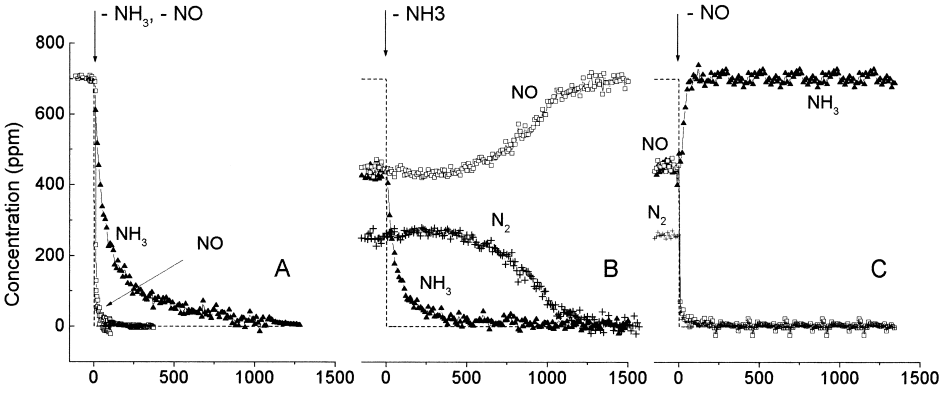

Fig. 8. Results of TRA performed over a V_2O_5–WO_3/TiO_2 model catalyst with V_2O_5=1.47% (w/w) and WO_3=9% (w/w). (A) Negative step addition of NO in He+O_2 and of NH_3 in He+O_2. (B) Negative step addition of NH_3 in He+NO+O_2. (C) Negative step addition of NO in He+NH_3+O_2. Experimental conditions: see Section 2. Dotted lines: ideal step; squares: NO; triangles: NH_3; crosses: N_2.

tracer (Ar) added to the feed (not shown in the figure). This clearly indicates that this species does not appreciably adsorb on the catalyst surface, in line with the results of the FT-IR investigation previously reported. A different situation is apparent in the case of ammonia (triangles). Indeed in this case upon the NH_3 positive inlet step (Fig. 7(A)) the ammonia reactor outlet concentration slowly changes with time and reaches the steady-state value only after several minutes. Along similar lines, when the NH_3 inlet concentration is decreased stepwise (Fig. 8(A)), the reactor outlet ammonia concentration slowly decreases with time. This clearly indicates that NH_3 is involved in adsorption–desorption processes on the catalyst surface.

Once the dynamics of the NH_3 and NO adsorption–desorption has been investigated, positive (Fig. 7(B) and (C)) and negative (Fig. 8(B) and (C)) stepwise changes in the NH_3 (or NO) reactor inlet concentrations have also been imposed in the presence of NO (or NH_3)+O_2. Fig. 7(B) and (C) show the typical results obtained over the ternary V_2O_5–WO_3/TiO_2 sample upon performing at t=0 s the switches NO→NO+NH_3 and NH_3→NH_3+NO in He+1% (v/v) O_2, respectively. The figures report the evolution with time of the ammonia, NO and N_2 concentrations.

Upon the NH_3 step feed (Fig. 7(B)), the NO reactor outlet concentration immediately decreases due to the occurrence of the SCR reaction, as also pointed out by the evolution of nitrogen and water (not reported in the figure) that is specular to the shape of NO consumption, thus indicating that the formation of these reaction products is not desorption-limited. No formation of other species (e.g. N_2O) was observed, in line with the occurrence of a genuine SCR process. The evolution with time of the ammonia and NO concentrations show different transient behaviors: the ammonia concentration profile exhibits a dead time (∼250 s) and then slowly increases with time on stream to the new steady-state value that is reached only after 800 s. On the other hand, the NO concentration trace does not show any dead time and rapidly decreases to its new steady-state value reached after ∼300 s.

A different transient behavior is observed upon the NO step feed in He+O_2+NH_3 (Fig. 7(C)). Also in this case upon the NO step feed (t=0 s) the NH_3 reactor outlet concentration immediately decreases due to the occurrence of the SCR reaction, as pointed out by the parallel evolution of N_2 and of water (not reported in the figure). The evolution with time on stream of ammonia, NO and N_2 concentrations upon the NO step feed significantly differs from those monitored during the corresponding NH_3 step feed experiments reported in Fig. 7(B). Indeed the concentrations of products and reactants reach their steady-state values almost immediately, in contrast to what was observed when the inlet NH_3 concentration was varied in a stepwise manner.

These results clearly indicate that NO is not involved in the adsorption–desorption processes on the catalyst surface, and are in line with an Eley–Rideal mechanism for the SCR reaction involving a

strongly adsorbed NH_3 species and a gas-phase or weakly adsorbed NO molecule.

The dynamics of the SCR reaction has also been investigated upon NH_3 and NO negative step changes (Fig. 8(B) and (C), respectively). In the case of the NH_3 shut-off (Fig. 8(B)), the NH_3 concentration rapidly decreases, whereas the NO and N_2 concentration signal are apparently not affected by the ammonia inlet step change for several minutes. Indeed only after ~600 s the NO concentration signal began to increase up to the inlet concentration value of 700 ppm, and correspondingly the N_2 and H_2O (not reported in the figure) concentration traces drop to zero. It is worthy to note that at the end of the transient experiment shown in Fig. 8(C) no NH_3 surface species were left on the catalyst surface, as demonstrated by TPD experiments performed at the end of the run. Hence, all the ammonia surface species initially present on the catalyst surface have been consumed in the SCR reaction. This point will be addressed later on.

A different situation is apparent upon the NO shut-off (Fig. 8(C)): indeed in this case the SCR reaction immediately stops after the NO switch. Again, the observed transient responses are typical of a reaction involving a strongly adsorbed species (NH_3) and a gas-phase or weakly adsorbed species (NO). Accordingly these results confirm that NO is not involved to a significant extent in adsorption–desorption processes on the catalyst surface, and are in line with the hypothesis of an Eley–Rideal mechanism for the SCR reaction.

The results of the NH_3+NO→NO switch reported in Fig. 8(B) show very interesting features of the reaction. Indeed it has been observed that the NO and N_2 concentrations do not change for several minutes in spite of the fact that the NH_3 reactor inlet concentration has been zeroed. This clearly indicates that ammonia adsorbed species are still available for the reaction, and that the rate of the SCR reaction does not depend on the ammonia surface concentration (θ_{NH_3}) for θ_{NH_3} values above a characteristic ''critical'' value, in line with the results of TPSR and TPR data previously reported (see above). The data reported above suggest that a ''reservoir'' or ''storage'' of adsorbed ammonia species available for the reaction is present on the catalyst surface, and also clearly indicates that the NH_3 adsorption sites differs from the NH_3 reactive sites. In particular, the results of the FT-IR investigation indicate that ammonia is adsorbed in the form of a molecularly coordinated NH_3 over Ti-, V- and W-sites, whereas NH_4^+ ions can be formed over V and W surface species (and on surface sulfates as well in the case of sulfate-containing catalysts). The estimates of the V, W and Ti surface coverages (θ_V, θ_W and θ_{Ti}, respectively) of the catalysts used in the transient response method experiments indicated that for the binary catalyst (V_2O_5=1.47% w/w) θ_V=0.21 and θ_{Ti}=0.79, whereas for the ternary sample (V_2O_5=1.47% w/w and WO_3=9% w/w) θ_V=0.12, θ_W=0.67 and θ_{Ti}=0.21. It is noted that in both catalysts the V coverage is limited, whereas Ti and W atoms predominate on the catalyst surface. The results of temperature programmed desorption/reaction studies and of FT-IR experiments performed with NH_3 and NH_3+NO showed that ammonia is strongly adsorbed over Ti and over TiO_2-supported V- and W-species, but that the reactivity in the SCR reaction of the surface V-, W- and Ti-oxide species is notably different [17,21,25,28]. Indeed the bare TiO_2 support is almost inert in the SCR reaction, whereas TiO_2-supported V- and W-oxides effectively convert NO, the reactivity of V being roughly one order of magnitude higher than that of W. Hence it can be concluded that the NO consumption is principally ascribed to the presence of vanadium only, whereas Ti-sites as well as V- and W-oxide species act as adsorption sites for ammonia. Accordingly these species act as an ammonia ''reservoir'' or ''storage'': as pointed out by the TRA this NH_3 storage can be involved in the SCR reaction upon ''migration'' (possibly in the gas-phase via desorption and re-adsorption) to near-by reactive V-sites, where NH_3 is consumed by gas-phase NO. In sulfur-containing catalysts, it is expected that sulfate species provide further stronger Brønsted acidity that can increase the capacity of the ammonia ''reservoir'' on the catalyst surface.

Results qualitatively similar to those reported in Figs. 7 and 8(A)–(C) have also been obtained at different temperatures (220–350°C) and over a binary V_2O_5/TiO_2 sample having the same vanadia loading (i.e. 1.47% w/w). However in the case of the binary catalyst sample lower NO conversions were measured at the same reaction temperatures if compared to the ternary catalyst, in line with the lower reactivity of the binary sample in the SCR reaction.

3.5. Mechanistic model of the SCR reaction

The data reported above pointed out a number of mechanistic features of the SCR reaction over V_2O_5–WO_3/TiO_2 catalyst samples that can be summarized as follows:

1. the reaction occurs between adsorbed ammonia and gas-phase or weakly adsorbed NO;
2. the catalyst active sites are the vanadium sites;
3. NH_3 is adsorbed on the catalyst surface both in the form of molecularly coordinated NH_3 (on V-, W- and Ti-sites) and of NH_4^+ ions (on V-, W-sites and on surface sulfates as well);
4. molecularly coordinated NH_3 species adsorbed on V-sites are activated in the SCR reaction possibly via the amide species whose presence has been observed in the FT-IR spectra;
5. ammonia species adsorbed on surface sites other than vanadium are not directly involved in the reaction but act as ammonia ''storage'' that can be consumed in the reaction after ''migration'' to reactive V-sites;
6. the mechanism is of the redox type, i.e. oxygen oxidizes the surface sites reduced by the other reactants.

Other well established mechanistic features of the reaction are (e.g. [29,30]):

1. the reaction stoichiometry is that of the above reaction (1);
2. the reaction is actually a coupling reaction, i.e. one N atom of the N_2 product comes from NO and the other from NH_3;
3. N_2O is not an intermediate.

Accordingly, on the basis of the data previously discussed and in agreement with the literature indications reported above, the mechanistic model for the SCR reaction over V_2O_5–WO_3/TiO_2 catalyst shown in Fig. 9 can be proposed. This mechanism, slightly modified with respect to that first reported by Ramis et al. [31], is referred to as the ''amide–nitrosamide'' mechanism, and consists of the following steps:

$$NH_{3(g)} + MO^{2-} \Leftrightarrow H_3N :\rightarrow MO^{2-} \quad (2)$$

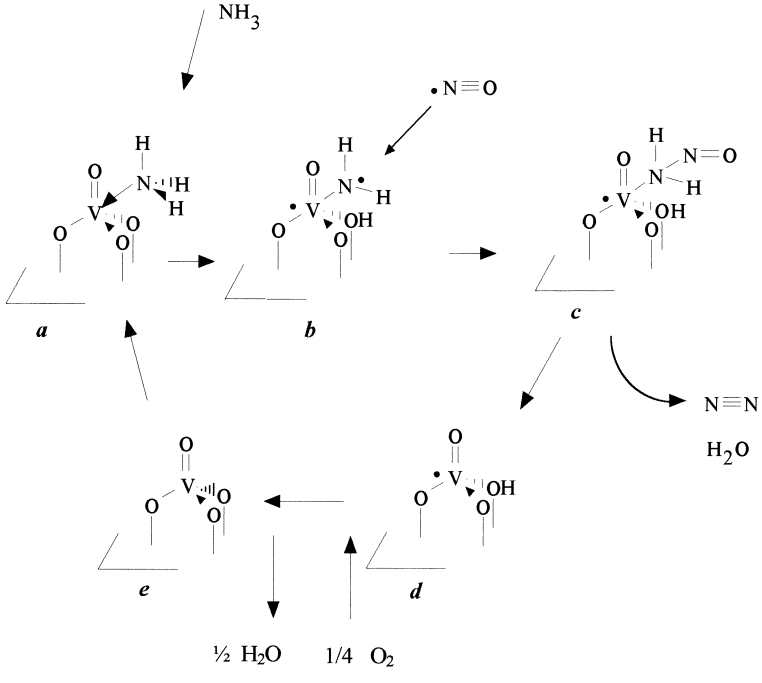

Fig. 9. Proposed ''amide–nitrosamide'' mechanism for the SCR over vanadia-based catalysts.

$$NH_{3(g)} + M{-}OH \Leftrightarrow MO^{-}NH_4^{+} \quad (3)$$

$$H_3N :\rightarrow V^{5+}O^{2-} \Rightarrow V^{4+}{-}NH_2 + {}^{-}OH \quad (4)$$

$$V^{4+}{-}NH_2 + NO \Rightarrow V^{4+}{-}NH_2NO \quad (5)$$

$$V^{4+}{-}NH_2NO \Rightarrow V^{4+} + N_2 + H_2O \quad (6)$$

$$2V^{4+} + \tfrac{1}{2}O_2 \Rightarrow 2V^{5+}{=}O \quad (7)$$

$$2OH^{-} \Rightarrow H_2O + O^{2-} \quad (8)$$

The first step of the reaction involves the reversible NH_3 adsorption on TiO_2-supported V- and W-species as well as on surface Ti-sites and sulfates (reactions (2) and (3)). These sites are denoted as MO^{2-} (Lewis acid sites) and M–OH (Brønsted acid sites). As shown by the FT-IR and transient experiments previously reported, only V-bonded molecularly adsorbed ammonia surface species (species *a* of Fig. 9 and of Scheme 3) has been considered as participating in the reaction, but ammonia held on Lewis or Brønsted Ti- and W-surface sites can also be involved in the reaction upon ''migration'' towards reactive V-sites. Accordingly, ammonia adsorbed over a Lewis V acid site is activated to an amide NH_2 species (reaction (4)), thus resulting in catalyst reduction. The activated ammonia species (species *b* of Fig. 9) then reacts with gas-phase NO (reaction (5)) giving rise to a nitrosamide intermediate species (species *c* of Fig. 9) which then decomposes to nitrogen and water (reaction (6)). The reduced catalyst sites are then regenerated by the gas-phase oxygen (reaction (7)). The proper sum of these equations gives the correct SCR reaction stoichiometry (1).

The proposed mechanism is the first one for vanadia-based catalyst implying an activation of ammonia on Lewis acid sites, but it is closely related to that previously proposed by Otto and Shelef [32] for metals and CuO_x. In addition to the reasons discussed above, other data support the ''amide–nitrosamide'' mechanism, e.g.:

1. nitrosamide NH_2NO was detected by mass spectrometry among the reaction products of SCR on vanadia-based catalysts [33] and traces of it were also found by IR spectroscopy at the catalyst surface [31];
2. several kinetic data can be successfully interpreted on the basis of this mechanism;
3. no ascertained published data contradict this mechanism;
4. this mechanism involves species that have examples in organometallic and inorganic chemistry and appears to be reasonable from the chemical point of view;
5. catalysts where Brønsted acidity is absent or very weak, such as CuO–TiO_2, MnO_x–TiO_2, Fe_2O_3–TiO_2, and Fe_2O_3 are also more or less active SCR catalysts [23].

The mechanism of the SCR reaction and the nature of the species potentially active have been investigated over vanadia-based catalysts by several authors since the 1970s. In particular, the debate concerning the role of Brønsted vs. Lewis acidity in the SCR mechanism is still open. However, the experiment described in Fig. 4 clearly shows that the Lewis-bonded ammonia species reacts with NO to give N_2, whereas on the other hand to our knowledge a clear result supporting a direct role of Brønsted sites in the SCR reaction has not been reported in the literature.

The present study also indicates that other catalyst functions are involved in the SCR reaction, which may play a crucial role in determining the catalyst reactivity. As a matter of fact, evidences have been provided in favor of a redox mechanism for the SCR reaction, and accordingly a key-role of the catalyst redox properties in the reactivity of the catalysts has been pointed out. The involvement of the catalyst redox properties has also been considered by other authors [10,15], who invoke the presence of two separate catalyst functions, i.e. a redox and an acid function, possibly associated to two adjacent sites [10]. Our data suggests that V-sites can carry both the oxidizing and the acid functionality that can work synergetically. Also, it is worth noting that other catalyst components, although inactive or poorly active in the SCR (e.g. the W and/or Ti surface sites), may have a role in the reaction. Indeed these species can strongly adsorb ammonia and accordingly they participate in the reaction as ''reservoir'' of adsorbed NH_3 species. These aspects may be of particular relevance in the case of samples having composition similar to that of commercial catalysts, i.e. very low V loading and high W and Ti surface coverage. Accordingly, a distinction should be made between the ammonia ''adsorption'' and ''reaction'' sites, and particularly when discussing

e.g. IR data of adsorbed ammonia (where the contribution of the bands arising from NH_3 adsorbed on the TiO_2 support are superimposed to those corresponding to the active sites) or in the derivation of kinetic models (NH_3 adsorption sites different from NH_3 reaction sites).

4. Conclusions

Combined chemico-physical and reactivity techniques have been used to probe the characteristics of commercial and home-made V_2O_5–WO_3/TiO_2 catalysts in the SCR reaction. The following conclusions can be drawn from our study:

1. The samples are constituted by TiO_2 anatase that supports the V and W components (and S in the case of commercial catalysts).
2. V, W and sulfates are present on the dry catalyst surface in the form of isolated vanadyl, wolframyl and sulfate species, all in a mono-oxo-type form. These species are strongly perturbed upon adsorption, thus showing that the above vanadyl and wolframyl sites can act as Lewis acid sites being formally coordinatively unsaturated.
3. NO does not adsorb on the catalyst surface, whereas NH_3 adsorbs over both Lewis and Brønsted acid sites. Lewis-bonded NH_3 species are thermally more stable than the ammonium ions, and upon heating a weak band is observed in the IR spectrum that has been assigned to an amide species NH_2.
4. The SCR reaction occurs between gas-phase or weakly adsorbed NO and ammonia bonded on Lewis acid sites, possibly via the amide species.
5. The mechanism is of the redox type, i.e. oxygen oxidizes the surface sites reduced by the other reactants.
6. NH_3 is adsorbed not only on the active V-sites but also on W- and Ti-sites and on surface sulfates as well. These sites are not very active in the SCR reaction and accordingly they act as ammonia ''reservoir'', that can be involved in the SCR reaction upon migration on active V-sites. It follows that a distinction should be made between ammonia ''adsorption'' and ''reaction'' sites.
7. On the basis of the mechanistic data obtained in the present study, and in line with other literature indications, a mechanistic model for the SCR reaction has been derived. This mechanism, referred to as the ''amide–nitrosamide'' mechanism, involves the activation of ammonia via an amide species that in turn can react with gas-phase NO leading to the formation of a nitrosamide intermediate. This intermediate then decomposes to N_2 and H_2O. Finally, the reduced catalyst active sites are reoxidized by gas-phase oxygen.

References

[1] S.M. Cho, Chem. Eng. Progr. 90 (1994) 39.
[2] P. Forzatti, L. Lietti, Heter. Chem. Rev. 3 (1996) 33.
[3] J.L. Alemany, L. Lietti, N. Ferlazzo, P. Forzatti, G. Busca, G. Ramis, E. Giamello, F. Bregani, J. Catal. 117 (1995) 155.
[4] L.J. Alemany, F. Berti, G. Busca, G. Ramis, D. Robba, G.P. Toledo, M. Trombetta, Appl. Catal. B 10 (1996) 299.
[5] J.P. Chen, R.T. Yang, Appl. Catal. A 80 (1992) 135.
[6] G. Deo, I.E. Wachs, J. Catal. 146 (1994) 335.
[7] V.I. Marshneva, E.M. Slavinskaya, O.V. Kalinkina, G.V. Odegova, E.M. Moroz, G.V. Lavrova, A.N. Salanov, J. Catal. 155 (1995) 171.
[8] V.M. Mastikhin, V.V. Terskikh, O.B. Lapina, S.V. Filimonova, M. Seidl, H. Knözinger, J. Catal. 156 (1995) 1.
[9] M.A. Vuurman, I.E. Wachs, A.M. Hirt, J. Phys. Chem. 95 (1991) 9928.
[10] I.E. Wachs, G. Deo, B.M. Weckhuysen, A. Andreini, M.A. Vuurman, M. de Boer, M.D. Amiridis, J. Catal. 161 (1996) 211.
[11] B.L. Duffy, H.E. Curry-Hyde, N.W. Cant, P.F. Nelson, J. Phys. Chem. 98 (1994) 7153.
[12] U.S. Ozkan, Y. Cai, M.W. Kumthekar, J. Phys. Chem. 99 (1995) 2363.
[13] G.T. Went, L.-J. Leu, R.R. Rosin, A.T. Bell, J. Catal. 134 (1992) 492.
[14] H. Schneider, S. Tschudin, M. Schneider, A. Wokaun, A. Baiker, J. Catal. 147 (1994) 5.
[15] N.-Y. Topsoe, J.A. Dumesic, H. Topsoe, J. Catal. 151 (1995) 241.
[16] L. Lietti, P. Forzatti, F. Bregani, Ind. Eng. Chem. Res. 35(11) (1996) 3884.
[17] L. Lietti, P. Forzatti, J. Catal. 147 (1994) 241.
[18] L. Lietti, I. Nova, S. Camurri, E. Tronconi, P. Forzatti, AIChE J. 43(10) (1997) 2559.
[19] D.C. Vermaire, P.C. van Berge, J. Catal. 116 (1989) 309.
[20] G.C. Bond, S.F. Tahir, Appl. Catal. 71 (1991) 1.
[21] L. Lietti, J.L. Alemany, P. Forzatti, G. Busca, G. Ramis, E. Giamello, F. Bregani, Catal. Today 29 (1996) 143.
[22] L. Lietti, J. Svachula, P. Forzatti, G. Busca, G. Ramis, F. Bregani, Catal. Today 17 (1993) 131.
[23] G. Ramis, L. Yi, G. Busca, M. Turco, E. Kotur, R.J. Willey, J. Catal. 157 (1995) 523.
[24] F. Kapteijn, L. Singoredjo, M. van Driel, A. Andreini, J.A. Moulijn, G. Ramis, G. Busca, J. Catal. 150 (1994) 105.

[25] L. Lietti, Appl. Catal. B 10 (1996) 281.
[26] L. Lietti, P. Forzatti, F. Berti, Catal. Lett. 41 (1996) 35.
[27] M.C. Paganini, L. Dell' Acqua, E. Giamello, L. Lietti, P. Forzatti, G. Busca, J. Catal. 166 (1997) 195.
[28] T.Z. Srnak, J.A. Dumesic, B.S. Clausen, E. Törnqvist, N.Y. Topsøe, J. Catal. 135 (1992) 246.
[29] F. Janssen, F. Van den Kerkhof, H. Bosch, J.R.H. Ross, J. Phys. Chem. 91 (1987) 5931.
[30] F. Janssen, F. Van den Kerkhof, H. Bosch, J.R.H. Ross, J. Phys. Chem. 91 (1987) 6633.
[31] G. Ramis, G. Busca, F. Bregani, P. Forzatti, Appl. Catal. 64 (1990) 259.
[32] K. Otto, M. Shelef, J. Catal. 18 (1970) 184.
[33] M. Farber, S.P. Harris, J. Phys. Chem. 88 (1984) 680.